The architecture of the IgG anti-carbohydrate repertoire in primary antibody deficiencies (PADs)

Tracking no: BLD-2019-001705R1-FINALFILES

Peter Jandus (University Hospital of Geneva, Switzerland) Kayluz Frias Boligan (University of Bern,) David Smith (Emory University School of Medicine, United States) Elisabeth de Graauw (University of Bern, Switzerland) Bodo Grimbacher (Satellite Center Freiburg, Germany) Camilla Jandus (University of Bern, Switzerland) Mai Abdelhafez (Modern Science and Art University (MSA), Egypt) Alain Despont (University of Bern, Switzerland) Nicolai Bovin (Auckland University of Technology, New Zealand) Dagmar Simon (Inselspital, Switzerland) Robert Rieben (University of Bern, Switzerland) Hans-Uwe Simon (University of Bern, Switzerland) Richard Cummings (Harvard Medical School, United States) Stephan von Gunten (Institute of Pharmacology, University of Bern, Switzerland)

Abstract:
Immune system failure in primary antibody deficiencies (PADs) has been linked to recurrent infections, autoimmunity and cancer, yet clinical judgment is often based on the reactivity to a restricted panel of antigens. Previously, we demonstrated that the human repertoire of carbohydrate-specific IgG exhibits modular organization related to glycan epitope structure. The current study compares the glycan-specific IgG repertoires among different PAD entities. Distinct repertoire profiles with extensive qualitative glycan-recognition defects were observed, characterized by the common loss of Galα- and GalNAc-reactivity and disease-specific recognition of microbial, self-antigens and tumor-associated carbohydrate antigens. Antibody repertoire analysis may provide a useful tool to elucidate the dimension and clinical implications of the immune system failure in individual patients.

Conflict of interest: No COI declared

COI notes:

Preprint server: No;

Author contributions and disclosures: S.V.G. and P.J. designed the study. K.F.B., P.J. and S.V.G. wrote the manuscript. K.F.B. and S.V.G. analyzed the data. Glycan array experiments at the CFG were conducted under supervision of D.F.S. and R.D.C. Database searches and computational analysis of the data set was performed by K.F.B. Patient sample collection, classification and preparation were done by B. G., C.J. and P.J. Experimental work was done by K.F.B., E.D.G., M.A., A.D. under supervision by D.S., H.U.S., R.R. and S.V.G. Glycan synthesis was supervised by N.B. All authors had full access to the data, helped draft the report or critically revised the draft, contributed to data interpretation, reviewed and approved the final version of the report.

Non-author contributions and disclosures: No;

Agreement to Share Publication-Related Data and Data Sharing Statement: emails to the corresponding author

Clinical trial registration information (if any):

The architecture of the IgG anti-carbohydrate repertoire in primary antibody deficiencies (PADs)

Running tittle: Carbohydrate-specific IgG repertoire in PAD

Author list: Peter Jandus[1†], Kayluz Frias Boligan[2†], David F. Smith[3], Elisabeth de Graauw[2], Bodo Grimbacher[4-7], Camilla Jandus[2,8,9], Mai M. Abdelhafez[10], Alain Despont[10], Nicolai Bovin[11,12], Dagmar Simon[13], Robert Rieben[10], Hans-Uwe Simon[2,14], Richard D. Cummings[3, 15], Stephan von Gunten[2]

[1]Division of Clinical Immunology and Allergy, Department of Internal Medicine, University Hospital and Faculty of Medicine, Geneva, Switzerland

[2]Institute of Pharmacology, University of Bern, Bern, Switzerland

[3]Emory Comprehensive Glycomics Core, Department of Biochemistry, Emory University School of Medicine, Atlanta, GA, USA

[4]Institute for Immunodeficiency, Center for Chronic Immunodeficiency (CCI), Medical Center, Faculty of Medicine, Albert-Ludwigs-University of Freiburg, Germany

[5]DZIF – German Center for Infection Research, Satellite Center Freiburg, Germany

[6]CIBSS – Centre for Integrative Biological Signalling Studies, Albert-Ludwigs University, Freiburg, Germany

[7]RESIST – Cluster of Excellence 2155 to Hanover Medical School, Satellite Center Freiburg, Germany

[8]Translational cytokine secreting lymphocyte group, Department of Oncology UNIL CHUV, University of Lausanne, Lausanne, Switzerland

[9]Ludwig Institute for Cancer Research, University of Lausanne, Lausanne, Switzerland

[10]Department for BioMedical Research (DBMR), University of Bern, Bern, Switzerland

[11]Shemyakin-Ovchinnikov Institute of Bioorganic Chemistry Russian Academy of Science, Moscow, Russian Federation

[12]Auckland University of Technology, Auckland, New Zealand

[13]Department of Dermatology, Inselspital, Bern University Hospital, University of Bern, Bern, Switzerland

[14]Department of Clinical Immunology and Allergology, Sechenov University, Moscow, Russia.

[15]Department of Surgery, Beth Israel Deaconess Medical Center, Harvard Medical School, Boston, Massachusetts, USA

31   Corresponding author: Stephan von Gunten, University of Bern, 3012 Bern,

32   Switzerland. Phone: 41-31-632-32-98; Fax: 41-31-632-49-94. E-mail:

33   stephan.vongunten@pki.unibe.ch

34

35

39   **Article length:** 3'818 words

40 **KEY POINTS:** Repertoire analysis by microarray technology constitutes a powerful

41 tool to evaluate immune system failure in PADs.

42

43

44 **ABSTRACT**

45 Immune system failure in primary antibody deficiencies (PADs) has been linked to

46 recurrent infections, autoimmunity and cancer, yet clinical judgment is often based on

47 the reactivity to a restricted panel of antigens. Previously, we demonstrated that the

48 human repertoire of carbohydrate-specific IgG exhibits modular organization related

49 to glycan epitope structure. The current study compares the glycan-specific IgG

50 repertoires among different PAD entities. Distinct repertoire profiles with extensive

51 qualitative glycan-recognition defects were observed, characterized by the common

52 loss of Galα- and GalNAc-reactivity and disease-specific recognition of microbial,

53 self-antigens and tumor-associated carbohydrate antigens. Antibody repertoire

54 analysis may provide a useful tool to elucidate the dimension and clinical implications

55 of the immune system failure in individual patients.

56

57 Abstract length: 114 words

58

59

60

61

62

63

64 **INTRODUCTION**

65   Inadequate humoral responses to carbohydrate-structures represent a

66 common feature of primary antibody deficiencies (PADs), despite the pathogenetic

67 heterogeneity of these disorders, involving monogenetic, polygenetic and still

68 unexplained defects[1,2]. These disorders are associated with a plethora of clinical

69 sequelae including severe and recurrent infections, microbial dysbiosis,

70 autoimmunity, allergy, granulomatous disease and malignancy[1,3,4].

71   The surface of all living cells is glycosylated, whereby the composition varies

72 between cell type[5], individuals, or species[6]. The prominent exposure of carbohydrate-

73 structures (glycans) on the surface of cells or bacterial capsules, renders them

74 accessible to antibodies, which facilitates the detection and elimination of pathogens

75 or aberrant cells, but also leads to adverse reaction in transfusion/transplantation

76 procedures (blood groups antigens), or to the acute rejection of xenografts (e.g. Gal-

77 α structures). Due to altered expression of biosynthetic enzymes, such as

78 glycosyltransferases or glycosidases, the glycome of cells is often changed under

79 pathological conditions, including cancer[7]. While tumor-associated carbohydrates

80 (TACAs) are exploited as diagnostic markers[8], there is also evidence for naturally-

81 occurring antibodies to TACAs in healthy individuals[9].

82   Insufficient responses to glycan-based vaccines or low titers of

83 isohemagglutinins, antibodies to polysaccharide blood group antigens, are

84 characteristic and diagnostic features of common variable immunodeficiency (CVID),

85 the most frequent symptomatic antibody deficiency diagnosed in adulthood[10,11].

86 Patients with specific antibody deficiency (SPAD) exhibit poor responses to structural

87 or capsular polysaccharides of bacteria (e.g. *S. pneumoniae, H. influenzae*), despite

88 the presence of normal serum concentrations of IgG, IgM and IgA[12]. Antibodies from

89   different IgG subclasses are known to contain different specificities for glycan-

90   structures[9,13], which may explain the predisposition of certain patients with IgG

91   subclass deficiency (IgGSD) to infections with encapsulated bacteria[12]. However,

92   current knowledge on the failure to raise adequate levels of glycan-specific

93   antibodies in PAD is mainly based on experience with specific bacterial antigens.

94   The clinical assessment of PADs by diagnostic vaccination (e.g.

95   pneumococcal vaccines, *S. typhi* Vi vaccine[14]) or the measurement of pre-existing

96   antibody titers (e.g. isohemagglutinins) relies on a restricted number of glycan

97   epitopes, thus providing only a narrow perspective of the actual dimensions of the

98   immunodeficiency. Further disadvantages of diagnostic vaccination include

99   diagnostic delay, laboratory-to-laboratory variation, serotype-specific responses, age

100   differences in antibody responses, or the challenging interpretation of

101   pre-immunization versus post-immunization specific antibody levels in patients not

102   receiving IgG replacement therapy[10,11,15-18]. The broader assessment of glycan-

103   specific antibodies in patients may better reflect the immune defect and also facilitate

104   treatment decisions, such as regarding life-long IgG replacement therapy.

105   Glycan array technology allows the high-throughput analysis of specific

106   antibody responses to carbohydrate antigens[19-21]. In a previous study using glycan

107   array version 5.1 of The Consortium for Functional Glycomics (CFG) to decipher the

108   IgG repertoire of healthy individuals we found that classes of glycans were

109   recognized with different intensity, depending on the terminal carbohydrate-moiety[9].

110   Here, we employed glycan array technology to investigate the IgG antibody repertoire

111   of PAD patients in terms of clinically relevant carbohydrate epitopes, including

112   microbial glycans, self- or xenoantigens, and TACAs.

MATERIALS AND METHODS

Study design

This non-randomized study was designed to investigate the human IgG anti-carbohydrate repertoire, in healthy and disease conditions, using glycan array technology combined with a computational system level approach. To this end, sera or purified IgG from healthy individuals or patients, as well as control antibodies were screened on microarrays by the Consortium for Functional Glycomics (CFG) or the US National Center for Functional Glycomics (NCFG).

Patient samples

Human blood was collected from healthy individuals (HD) or patients upon informed and written consent in accordance with the Declaration of Helsinki. All experimental protocols were approved by the local institutional and/or licensing committees (KEK-BE: 148/10 and KEK No. 224/01). Therapeutic naïve patients followed at the University Hospital of Bern from January 2005 to December 2011 were retrospectively identified. Additional sera of therapeutic naïve patients without IgG replacement therapy were provided from B.G. CVID was defined in accordance with the criteria of the Pan-American Group for Immunodeficiency and the European Society for Immunodeficiency[22]. Inclusion criteria for IgGSD were a normal total IgG concentration with a significant decrease (more than two standard deviations below the mean for the age) in the serum concentrations of one or more IgG subclasses[23] with recurrent episodes of infection. Symptomatic hypogammaglobulinemia (HGG) was defined with decreased total IgG concentration, but not fulfilling criteria for CVID with respect to a reduction of two immunoglobulin isotypes and/or reduced response to vaccination. For diagnostic vaccination the pneumococcal polysaccharide vaccine

137 (PPV) Pneumovax-23 (MSD, Lucerne, Switzerland) was used in patients with IgG

138 levels at or higher than 4 g/L. Levels of pneumococcal capsular polysaccharide

139 (PCP) IgG > 50 mg/L and for PCP IgG2 > 40 mg/L were considered as normal. A

140 sufficient PPV vaccination response was defined as PCP titers above these levels

141 and/or PCP IgG and IgG2 levels above 100 mg/L and/or a 4-fold increase of post-

142 vaccination PCP IgG and PCP IgG2 titers as detected 4 to 6 weeks after vaccination.

143 SPAD was diagnosed in patients with normal total immunoglobulin and IgG subclass

144 concentrations but impaired pneumococcal polysaccharide vaccine (PPV) response.

145 The characteristics of the different groups are summarized in Table S1. Patients were

146 not stratified for specific infections. The sera from these patients were individually

147 screened in the NCFGv2 glycan array or pooled in the indicated groups and

148 screened in the CFG glycan array. IgG purification was performed by affinity

149 chromatography in Ab SpinTrap columns (GE Healthcare). Pooled sera from patients

150 and healthy donors were directly applied to the columns and the purification

151 procedures performed according to manufacturer instructions. The control IgG

152 preparation (IgG control mix) was prepared by mixing two monoclonal human

153 myeloma proteins, IgG1λ (67%) and IgG2κ (33%), purchased from Sigma-Aldrich.

154 This process resulted in a κ/λ ratio of 0.5, which is well within the range found in

155 normal serum (0.26 to 1.65). The concentration of IgG in the different samples was

156 determined using a Behring Turbitimer instrument (Dade Behring). The quality of the

157 isolated antibodies was checked by SDS-PAGE under reducing and non-reducing

158 conditions (Figure S1).

159 **Glycan array analysis**

160 The glycan microarrays from the CFG

161 (http://www.functionalglycomics.org/static/consortium/resources/resourcecoreh8.shtm

162 l) were prepared from amine functionalized glycan structures covalently coupled in

163 microarrays to N-hydroxysuccinimide-derivatized microscope slides as previously

164 described[24]. On NCFG array version 2 (NCFGv2) carbohydrates were conjugated

165 with the fluorescent linker AEAB, by reductive amination with sodium

166 cyanoborohydrate to form glycan-AEABs (GAEABs). For both arrays, the human sera

167 or purified IgG or IgG control mix, were identically processed and screened at

168 180µg/ml using a secondary biotinylated anti-human IgG mAb (clone HP-6043) at 5

169 µg/ml followed by Alexa633-coupled streptavidin[9]. A positive streptavidin control was

170 used. Sample preparation and analysis was performed as indicated on the CFG

171 website (www.functionalglycomics.org). To determine the specific binding to selected

172 glycans, the antibody binding ratio (ABR) was calculated. The computed ABR

173 represents the quotient of the respective sample relative fluorescent units (RFU) and

174 the corresponding IgG control mix RFU. Data are expressed as the mean of RFU or

175 ABR values from six repeated experiments, if not indicated otherwise.

176 **Database search**

177 The identity or characteristics of glycans was investigated by consulting the

178 databases of the Consortium of Functional Glycomics

179 (http://www.functionalglycomics.org/fg/)   or   PubMed

180 (http://www.ncbi.nlm.nih.gov/pubmed/guide/). The online Bacterial Carbohydrate

181 Structure Data Base (BCSDB) was consulted to identify the bacterial origin of the

182 glycans (http://csdb.glycoscience.ru/bacterial/).

183 **Statistical analysis**

184 Correlation matrixes, heatmaps and hierarchical clustering were performed using "R"

185 (The R Foundation for Statistical Computing, Version 3.0.2)[25]. Representation of the

186   data was done using the function heatmap.2 from the package *gplots*[26]. Hierarchical

187   clustering and dendrograms were calculated with the complete method of the hclust

188   function. Statistical analysis and other illustrations were performed using Microsoft

189   Excel (Microsoft Corporation, 2011, Version 14.0.0) and GraphPad PRISM

190   (Graphpad Software, Inc., Version 6.0c). For clique distribution analysis, only groups

191   with common terminal carbohydrate moiety that are represented at least with 12

192   glycans (2% of total) on CFG glycan array version 5.1 were taken into consideration.

193   For statistical analysis, Kruskal-Wallis, Student's *t*-test, Spearman correlation and

194   Two-way ANOVA tests were used. Given the small size of the group (n=2), the CVID

195   PPV^{low} subset on the NCFGv2 array was excluded when group comparisons were

196   performed.

197

198   Further methods are available in the supplemental data, available on the *Blood* Web

199   site.

200   For original data, please contact the corresponding author.

201

202 **RESULTS**

203 **Broad carbohydrate reactivity defects (CRD) in diverse PAD entities**

204 Sera from PAD patients or healthy donors (HD) were screened on CFG glycan array

205 version 5.1 to analyze the IgG binding reactivity to 610 distinct glycans at 180µg/ml.

206 In accordance with previous reports[9,13] this assay concentration was determined to

207 be optimal, resulting in reproducible IgG glycan-binding patterns with minimal

208 background. Cohorts included patients with symptomatic hypogammaglobulinemia

209 (HGG n=76), SPAD (n=5) or IgG subclass deficiency (IgGSD; n=8), CVID (n=25),

210 CVID with low PPV vaccination response (CVID PPV[low]; n=6) or HD (n=43).

211 Using this platform, we observed broad IgG reactivity to printed glycans in

212 pooled sera from healthy donors (Fig. 1A; Table S2), which is consistent with

213 previously published data[9,13,21,27-29]. In contrast, marked reduction of overall glycan

214 binding intensities was observed for all investigated PAD patient subsets, with lowest

215 averaged relative fluorescence units (RFU) in CVID, particularly in CVID PPV[low]

216 patients (Fig. 1A). Next, IgG was purified from CVID, HGG and healthy donor sera by

217 affinity chromatography, and then screened on glycan array. As with whole sera, anti-

218 glycan reactivity of equimolar, purified IgG from immunocompromised patients

219 presented lower RFU values on average compared to healthy controls (Fig. S1).

220 In an effort to compare the carbohydrate-specific IgG repertoires between

221 PAD patients and healthy subjects, individual sera were screened. To this end glycan

222 array version 2 from the US National Center of Functional Glycomics (NCFGv2)

223 containing 147 glycans was used, which allowed us to include more samples.

224 Identical glycans were similarly recognized on both arrays (Fig. S2). Figure 1B

225 illustrates the computed reactivity matrix (mean RFU values) ordered by a

226 dendrogram clustering algorithm[30]. Columns represent the antibody reactivity profiles

227 (reactivity of each specific glycan for the different sera samples), and the rows reflect

228 the immune profiles for each patient subgroup. The dendrogrammed reactivity matrix

229 illustrates the broader spectrum of glycan reactivity in healthy donor sera compared

230 to all screened PAD patient subgroups, yet revealing a similar binding profile as

231 compared to the SPAD cohort. The glycan-binding profiles of IgGSD, HGG and CVID

232 sera displayed a narrower spectrum of glycan reactivity, which was most impaired in

233 the CVID subgroup. CVID and CVID PPV[low] patients also exhibited the lowest

234 averaged RFU values (Fig. S2). No clear clustering of individual immunoprofiles was

235 observed for total glycans, which was expected as the arrays contain synthetic

236 glycans without known biological relevance (Fig. S2).

237 **Glycan-specific IgG antibodies to bacterial antigens in PAD**

238 PADs are characterized by recurrent, severe or unusual bacterial infections,

239 especially by bacteria protected by a polysaccharide capsule. Thus, we decided to

240 analyze the IgG reactivity profiles to known bacterial carbohydrates. On glycan array

241 CFG version 5.1, we previously identified 121 bacterial carbohydrate antigens

242 consulting the Bacterial Carbohydrate Structure Data Base (BCSDB)[9], providing a

243 platform for high-throughput analysis for antibody reactivity to carbohydrate epitopes

244 of multiple bacterial species. The printed glycans include capsular and structural

245 oligosaccharides, as well as exopolysaccharides of commensal and pathogenic

246 bacterial species[9]. In comparison to immunoprofiles of healthy subjects, Spearman's

247 rank correlation analysis revealed divergent IgG reactivity profiles to bacterial glycan

248 epitopes in PAD cohorts, with the lowest correlation of 0.34 CVID PPV[low] patients and

249 0.57 for CVID, when pooled sera were screened on the CFG array (Fig. 2A). Figure

250 2B illustrates the collective reactivity matrix (mean RFU values) of individual sera to

251 65 bacterial glycans on the NCFGv2 array. Hierarchical clustering analysis revealed

252   a substantial loss of reactivity for the IgGSD, HGG and CVID cohorts. An extensive

253   reduction of anti-bacterial reactivity was also found for recognition of the majority of

254   121 bacterial glycans on the CFG array version 5.1 in pooled sera from patients in

255   these cohorts (Fig. S3). No clear clustering of individual immunoprofiles was

256   observed for bacterial glycans, which may be due to differential natural exposure to

257   bacteria (Fig. S3).

258   The glycan array technology combined with the consultation of the BCSDB

259   databank allowed to screen in parallel several distinct epitopes that were identified as

260   glycan constituents of specific bacteria. Figure 2C shows individual profiles of IgG

261   reactivity to glycans on the NCFGv2 array that are found in *E. coli* (glycans: n=15), *H.*

262   *pylori* (n=15), *N. meningitidis* (n=6), *H. influenzae* (n=3), *S. pneumoniae* (n=2), and

263   *Salmonella* (n=2) species. Heterogenous immunoprofiles were observed in all

264   cohorts, including healthy individuals. However, reactivity profiles were particularly

265   low in CVID and CVID PPV^{low}, who exhibited a significant loss of IgG antibodies

266   specific for pathogens and commensals, including antigens to which human beings

267   are frequently exposed and immunized. Missing antibodies against Neisseria

268   meningitis and Salmonella in the different groups may reflect lack of exposure to

269   these pathogens.

Recognition of TACA and Siglec ligands in PAD

271   One life-threatening complication of PAD, in particular of CVID, is the

272   occurrence of malignancies[1,31-34]. Since altered surface glycosylation is a hallmark of

273   cancer and influences different aspects of tumor progression and anti-tumor

274   immunity[7,35,36], we set out to explore IgG reactivity to tumor-associated carbohydrate

275   antigens. Figure 3A demonstrates the IgG reactivity profiles to twenty-two glycan

276   epitopes on CFG glycan array version 5.1 that constitute well-established TACAs. In

277   accordance with our previous data[9], healthy donor sera contained natural antibodies

278   against TACAs. High reactivity was found against Lewis antigen-related TACAs,

279   gangliosides, Thomsen-Friedenreich (TF) and globo-series-associated antigens.

280   Loss of anti-TACA IgG reactivity was found in all examined PAD patient subgroups.

281   The reduced binding activity by IgG was most dominant in CVID PPV[low] donors,

282   followed by CVID patients, as computed based on RFU profiles and represented as

283   circular dendrogram (Fig. 3B). To further explore these findings we analyzed anti-

284   TACA signatures of individual sera screened on the NCFGv2 array. Most sera from

285   healthy individuals exhibited high anti–TACA reactivity to Forssman antigen,

286   Globoside, Globo H and SSEA-4 hexaose, but heterogenous binding to other TACAs

287   (Fig. 3C). The substantial loss of anti-TACA reactivity in CVID was confirmed in

288   individual sera. In contrast, antibody binding to the Forssman antigen was found in all

289   cohorts and all screened individual sera (Fig. 3A and C), indicating that this glycan-

290   epitope is highly immunogenic with widely maintained specific antibody production in

291   the PAD patients. Indeed, in the CVID PPV[low] and some CVID patients, Forssman

292   antigen was the only investigated TACA for which higher intensity signals were

293   detected. Reactivity to GM1 was particularly low in CVID patients. This is remarkable

294   as GM1 expression is present and positively correlates with rituximab treatment

295   response in non-Hodgkin's lymphoma[37], which is among the most frequent

296   malignancies occurring in these patients[10].

297   Overexpression of sialylated TACAs frequently occurs in tumors and

298   hypersialylation has been linked to tumor progression and immune escape by the

299   engagement of inhibitory Siglec receptors on leukocytes[7,36,38-40]. In PAD cohorts the

300   antibody recognition of certain sialoglycans with known Siglec binding capacity was

301   similar or reduced on the glycan array compared to healthy donor responses (Fig.

302   S4). However, for two ligands of CD22/Siglec-2, expressed on B cells, binding was

303 high (# 377) or even increased (# 268). Little is known about the tissue expression of

304 these two ligands and it remains to be shown if such antibodies at higher levels might

305 interfere with the CD22 receptor / ligand axis to unleash B cell responses under

306 certain circumstances.

307 **Failure to raise Galα- and GalNAc-directed IgG antibodies in PAD**

308 The composition of glycan antigens, in particular the terminal carbohydrate-

309 moiety, has been linked to the immunogenicity of a given glycan in healthy

310 individuals[9]. This raised the question about the effect of the relationship between

311 immune system failure (ISF) in PAD subgroups and the structure-related

312 immunogenicity on the architecture of the glycan-specific IgG repertoire. A binary

313 deviation matrix was computed considering statistical deviation ($P < 0.05$) of IgG

314 binding (RFU values) for each PAD cohort and each glycan compared to healthy

315 donor data and reordered by a dendrogram clustering algorithm (Fig. 4A). The rows

316 in this matrix indicate the binary antibody reactivity profiles, and the columns

317 represent the deviation immune profiles for each PAD subgroup. By hierarchical

318 clustering analysis four major subgroups were identified: predominant were clique 4

319 representing glycans with deviation in all PAD cohorts (n=293; 48%) and clique 2

320 containing glycans without deviation in all PAD cohorts (n=245; 40%); of lower

321 magnitude were clique 1 (n=5; 1%) and clique 3 (n=67; 11%) encompassing glycans

322 with heterogeneous IgG binding activities between subgroups (Table S3).

323 Given the association between immunogenicity and terminal carbohydrate

324 moiety of glycans[9,41], the clique distribution of glycans was investigated based on

325 their structure. The most dominant deviation was found for Galα- and GalNAc-

326 terminated glycans (Fig. 4B). Forty-seven (85.5%) versus only one (1.8%) Galα-

327 structure(s), and 37 (68.5%) versus 12 (22.2%) GalNAc-terminated glycans were

328   represented in clique 4 or clique 2, respectively. In accordance, the IgG antibody-

329   binding levels (RFU values) of Galα- and GalNAc-terminated glycans were lower in

330   all cohorts (Fig. 4C, D). In depth analysis computing a deviation matrix based on *P*

331   values and hierarchical clustering analysis revealed large glycan clusters that were

332   concomitantly either non-aberrant (clique B) or aberrant (clique E) for all disease

333   entities compared to healthy individuals (Fig. 4E), whereby Galα- (70.9%) and

334   GalNAc- (62.9%) terminated glycans were most prevalent in clique E (Fig. 4F),

335   indicating failed antibody responses to these specific structures.

336   As a consequence of the inactivation of the *GGTA1* gene encoding for

337   α1,3galactosyltransferase (GalT), humans, apes and Old World monkeys do not

338   express the Galili epitope Galα1-3Galβ1-4GlcNAcβ[39]. Natural antibodies to this

339   xenoantigen in most humans, eventually generated in response to the microbiota of

340   the host, are considered a key factor in the rejection of xenografts[43], and

341   necessitated the development of GalT knockout (GalTKO) animals[44,45]. Using a

342   suspension array, we examined individual sera from patients (HGG, n=37; CVID,

343   n=15; IgGSD, n=8) and healthy donors (n=18) for IgG reactivity to the Galili epitope

344   and other Galα- and GalNAc-terminated structures including, αLN (Galα1-

345   4GlcNAcβ), Aα3GN (Galα1-3GlcNAcβ), or A and B blood group antigens (Fig. 5A

346   and S5). Low isohemagglutinins are frequently observed in CVID patients[11].

347   Consistent with this observation, we found reduced IgG reactivity to blood group A

348   and B antigens also in the HGG, SPAD and IgGSD cohorts (Fig. S6). The IgG

349   reactivity to Galα- and GalNAc-terminated epitopes was consistently lower in most

350   PAD patients, whereby the reduction was most significant for the Galili epitope, as

351   evidenced by statistical analysis (Fig. 5A and S5).

352   Given the significant loss of anti-Galili reactivity in PAD patients, functional

353 implications were tested in a xenoreactivity assay, analyzing antibody-dependent cell

354 cytotoxicity (ADCC) of primary human natural killer (NK) cells directed against the

355 porcine kidney cell line PK15. On this cell line the Galili epitope is highly expressed

356 on the surface and lost following enzymatic digestion by α-galactosidase as

357 assessed by flow cytometry (Fig. 5B). Sera from healthy donors induced substantial

358 NK cell-mediated ADCC activity against the Galili-positive PK15 cells, which was

359 abolished following α-galactosidase treatment of the porcine target cells (Fig. 5C),

360 illustrating the dependence of the xenogeneic activity on Gal-α epitopes, including

361 Galili. In contrast, CVID sera failed to promote NK cell-mediated ADCC against the

362 porcine Galili-positive target cells at equimolar IgG concentrations (1mg/mL),

363 indicating a repertoire defect for the recognition of xenogeneic antigens. Moreover,

364 the loss of the xenogeneic potential of CVID sera was demonstrated in a modified

365 version of an established model for antibody-mediated skin damage[46,47], involving

366 cryosections of porcine skin incubated with patients' sera and leukocytes from

367 healthy donors and the assessment of dermal-epidermal separation. Porcine skin

368 damage was significantly lower in the presence of CVID sera compared to human

369 control sera at equimolar IgG concentrations (Fig. 5D). Together, these data provide

370 evidence for humoral immune system failure beyond quantitative antibody deficiency,

371 which involves repertoire defects in PAD.

372

DISCUSSION

The emerging picture is that the human IgG anti-carbohydrate repertoires in health[9], and in primary antibody deficiencies, exhibit a modular organization, yet with a different architecture in PAD. Translated to Cohen's concept of immune computation[48], our data imply that primary antibody deficiency is not solely characterized by aberrant antibody production, but features disturbed immune-system response states (the output) due to an altered algorithm to compute immunogenic states (the input) that is dictated by impaired cellular and molecular networks of innate and adaptive immunity[49,50].

Despite the heterogeneous genetic basis across PAD entities[1], deviation mapping revealed significant repertoire similarities pointing toward a common disease-modifying algorithm that drives humoral immune system failure. Dominant was the reduced or lost specificity for Galα– or GalNAc-terminated glycan epitopes in PAD patients, for which healthy individuals express high levels of naturally occurring antibodies, eventually in response to immune stimulation by carbohydrate antigens of their microbiota[9,41]. The loss of Galα– or GalNAc-specific antibodies might thus reflect the lost capacity to induce these antibodies in response to the host microbiota, or reflect the microbial dysbiosis in PAD[4], or both. Interestingly, bacteria and tumor cells use certain glycosylation patterns to escape immunity, such as sialoglycans that engage inhibitory Siglec receptors on leukocyte subsets of myeloid and lymphoid lineages[6,35,39,40,51]. It remains to be shown if naturally-occurring antibodies to TACA are also induced by the microbiota and if the observed loss has consequences for PAD patients. Notably, the loss of IgG reactivity to tumor antigens was most evident in the CVID cohort, a disorder in which the incidence of malignancy is increased[10], supporting the concept of aberrant immune surveillance in PID[52]. For instance, we

398 observed low antibody reactivity to TACAs known to be expressed on CVID-

399 associated malignancies, such as GM1 in non-Hodgkin's lymphoma[37], or Thomson-

400 Friedenreich antigen in gastric cancer[53,54]. However, tumor glycosylation patterns and

401 their immunoreactivity remain to be fully explored for CVID-associated malignancies.

402 Glycoimmunology remains a relatively underdeveloped field and the need for

403 interdisciplinary collaborations and the enhanced training of glycoscientists in

404 biomedical areas has been identified[55]. In line with this, there is also a demand for

405 tools, such as glycan arrays, the development of which is challenging given the

406 availability of differently synthesized or purified glycans. However, this initial study

407 highlights the potential and the need to expand glycan array studies in PAD using

408 biological samples from larger patient cohorts. Clusters of glycans were identified

409 with different reactivity profiles between PAD subgroups (cliques 3, A, C, D), which

410 may be candidates for diagnostic use. In future studies, it will also be advisable to

411 compare glycan-specific antibody profiles with clinical and laboratory parameters

412 (e.g. switched memory B cell numbers, blood groups), and in specifically classified

413 patient subsets[56].

414 The broad and qualitative assessment of the immune system failure (ISF) in

415 individual patients may be informative regarding the severity of the disease,

416 eventually leading to more personalized treatment decisions. Glycan array

417 technology may thus provide a useful option for the individual assessment of ISF and

418 facilitate clinical practice, especially given the heterogeneity of PAD entities with a

419 growing list of identified pathogenetic defects[2]. However, our broad analysis

420 demonstrates the extent of the skewed IgG repertoire with impaired reactivity to

421 biologically relevant glycan epitopes, including those linked to PAD-associated

422 clinical manifestations, such as infection, malignancy and autoimmunity[1,10]. Our

423 systems immunology approach highlights the power of high-throughput assessment

424 of humoral immune system failure by microarray technology, which may have

425 potential ramifications for the diagnosis, classification and therapy of PAD patients.

426

443

444 **AUTHORSHIP**

445 **Contributions:** S.V.G. and P.J. designed the study. K.F.B., P.J. and S.V.G. wrote

446 the manuscript. K.F.B. and S.V.G. analyzed the data. Glycan array experiments at

447 the CFG were conducted under supervision of D.F.S. and R.D.C. Database searches

448   and computational analysis of the data set was performed by K.F.B. Patient sample

449   collection, classification and preparation were done by B. G., C.J. and P.J.

450   Experimental work was done by K.F.B., E.D.G., M.A., A.D. under supervision by

451   D.S., H.U.S., R.R. and S.V.G. Glycan synthesis was supervised by N.B. All authors

452   had full access to the data, helped draft the report or critically revised the draft,

453   contributed to data interpretation, reviewed and approved the final version of the

454   report.

455   **Conflict-of-interest disclosure:** The authors declare no competing financial

456   interests.

457   *Correspondence: Stephan von Gunten, Institute of Pharmacology, University of

458   Bern, Inselspital INO-F, CH-3010 Bern, Switzerland; e-mail:

459   stephan.vongunten@pki.unibe.ch

460   **FOOTNOTES**

461   †P.J. and K.F.B. contributed equally to this publication

462

463

464

465

466

467

468

REFERENCES

1. Durandy A, Kracker S, Fischer A. Primary antibody deficiencies. *Nat Rev Immunol*. 2013;13(7):519-533.

2. Bousfiha A, Jeddane L, Picard C, et al. The 2017 IUIS phenotypic classification for primary immunodeficiencies. *J Clin Immunol*. 2018;38(1):129-143.

3. Verma N, Grimbacher B, Hurst JR. Lung disease in primary antibody deficiency. *Lancet Respir Med*. 2015;3(8):651-660.

4. Berbers RM, Nierkens S, van Laar JM, Bogaert D, Leavis HL. Microbial dysbiosis in common variable immune deficiencies: evidence, causes, and consequences. *Trends Immunol*. 2017;38(3):206-216.

5. North SJ, von Gunten S, Antonopoulos A, et al. Glycomic analysis of human mast cells, eosinophils and basophils. *Glycobiology*. 2012;22(1):12-22.

6. Adams OJ, Stanczak MA, von Gunten S, Laubli H. Targeting sialic acid-Siglec interactions to reverse immune suppression in cancer. *Glycobiology*. 2017.

7. Boligan KF, Mesa C, Fernandez LE, von Gunten S. Cancer intelligence acquired (CIA): tumor glycosylation and sialylation codes dismantling antitumor defense. *Cell Mol Life Sci*. 2015;72(7):1231-1248.

8. Stowell SR, Ju T, Cummings RD. Protein glycosylation in cancer. *Annu Rev Pathol*. 2015;10:473-510.

9. Schneider C, Smith DF, Cummings RD, et al. The human IgG anti-carbohydrate repertoire exhibits a universal architecture and contains specificity for microbial attachment sites. *Sci Transl Med*. 2015;7(269):269ra261.

10. Bonilla FA, Barlan I, Chapel H, et al. International consensus document (ICON): common variable immunodeficiency disorders. *J Allergy Clin Immunol Pract*. 2016;4(1):38-59.

11. Orange JS, Ballow M, Stiehm ER, et al. Use and interpretation of diagnostic vaccination in primary immunodeficiency: a working group report of the Basic and Clinical Immunology Interest Section of the American Academy of Allergy, Asthma & Immunology. *J Allergy Clin Immunol*. 2012;130(3 Suppl):S1-24.

12. Fried AJ, Bonilla FA. Pathogenesis, diagnosis, and management of primary antibody deficiencies and infections. *Clin Microbiol Rev*. 2009;22(3):396-414.

13. von Gunten S, Smith DF, Cummings RD, et al. Intravenous immunoglobulin contains a broad repertoire of anticarbohydrate antibodies that is not restricted to the IgG2 subclass. *J Allergy Clin Immunol*. 2009;123(6):1268-1276 e1215.

14. Evans C, Bateman E, Steven R, et al. Measurement of Typhi Vi antibodies can be used to assess adaptive immunity in patients with immunodeficiency. *Clin Exp Immunol*. 2018;192(3):292-301.

15. Daly TM, Hill HR. Use and clinical interpretation of pneumococcal antibody measurements in the evaluation of humoral immune function. *Clin Vaccine Immunol*. 2015;22(2):148-152.

507   16. Ballow M. Vaccines in the assessment of patients for immune deficiency. *J Allergy Clin*
508   *Immunol*. 2012;130(1):283-284 e285.

509   17. Gelfand EW, Ochs HD, Shearer WT. Controversies in IgG replacement therapy in patients
510   with antibody deficiency diseases. *J Allergy Clin Immunol*. 2013;131(4):1001-1005.

511   18. Perez E, Bonilla FA, Orange JS, Ballow M. Specific antibody deficiency: controversies in
512   diagnosis and management. *Front Immunol*. 2017;8:586.

513   19. Grader-Beck T, Boin F, von Gunten S, Smith D, Rosen A, Bochner BS. Antibodies recognising
514   sulfated carbohydrates are prevalent in systemic sclerosis and associated with pulmonary
515   vascular disease. *Ann Rheum Dis*. 2011;70(12):2218-2224.

516   20. Campbell CT, Gulley JL, Oyelaran O, Hodge JW, Schlom J, Gildersleeve JC. Humoral
517   response to a viral glycan correlates with survival on PROSTVAC-VF. *Proc Natl Acad Sci U S*
518   *A*. 2014;111(17):E1749-1758.

519   21. Stowell SR, Arthur CM, McBride R, et al. Microbial glycan microarrays define key features of
520   host-microbial interactions. *Nat Chem Biol*. 2014;10(6):470-476.

521   22. Conley ME, Notarangelo LD, Etzioni A. Diagnostic criteria for primary immunodeficiencies.
522   Representing PAGID (Pan-American Group for Immunodeficiency) and ESID (European
523   Society for Immunodeficiencies). *Clin Immunol*. 1999;93(3):190-197.

524   23. Al-Herz W, Bousfiha A, Casanova JL, et al. Primary immunodeficiency diseases: an update on
525   the classification from the international union of immunological societies expert committee for
526   primary immunodeficiency. *Front Immunol*. 2011;2:54.

527   24. Blixt O, Head S, Mondala T, et al. Printed covalent glycan array for ligand profiling of diverse
528   glycan binding proteins. *Proc Natl Acad Sci U S A*. 2004;101(49):17033-17038.

529   25. R Core Team. R: A language and environment for statistical computing. R Foundation for
530   Statistical Computing, Vienna, Austria. URL https://www.R-project.org/ 2019.

531   26. Warnes GR, Bolker B, Bonebakker L, et al. gplot: Various R Programming Tools for Plotting
532   Data. URL http://cran.r-project.org/package=gplots 2015.

533   27. Padler-Karavani V, Yu H, Cao H, et al. Diversity in specificity, abundance, and composition of
534   anti-Neu5Gc antibodies in normal humans: potential implications for disease. *Glycobiology*.
535   2008;18(10):818-830.

536   28. Pashov A, Monzavi-Karbassi B, Kieber-Emmons T. Immune surveillance and immunotherapy:
537   lessons from carbohydrate mimotopes. *Vaccine*. 2009;27(25-26):3405-3415.

538   29. Huflejt ME, Vuskovic M, Vasiliu D, et al. Anti-carbohydrate antibodies of normal sera: findings,
539   surprises and challenges. *Mol Immunol*. 2009;46(15):3037-3049.

540   30. Madi A, Hecht I, Bransburg-Zabary S, et al. Organization of the autoantibody repertoire in
541   healthy newborns and adults revealed by system level informatics of antigen microarray data.
542   *Proc Natl Acad Sci U S A*. 2009;106(34):14484-14489.

543   31. Kinlen LJ, Webster AD, Bird AG, et al. Prospective study of cancer in patients with
544   hypogammaglobulinaemia. *Lancet*. 1985;1(8423):263-266.

545 32. Chapel H, Lucas M, Lee M, et al. Common variable immunodeficiency disorders: division into
546   distinct clinical phenotypes. *Blood*. 2008;112(2):277-286.

547 33. Resnick ES, Moshier EL, Godbold JH, Cunningham-Rundles C. Morbidity and mortality in
548   common variable immune deficiency over 4 decades. *Blood*. 2012;119(7):1650-1657.

549 34. Vajdic CM, Mao L, van Leeuwen MT, Kirkpatrick P, Grulich AE, Riminton S. Are antibody
550   deficiency disorders associated with a narrower range of cancers than other forms of
551   immunodeficiency? *Blood*. 2010;116(8):1228-1234.

552 35. Fuster MM, Esko JD. The sweet and sour of cancer: glycans as novel therapeutic targets. *Nat
553   Rev Cancer*. 2005;5(7):526-542.

554 36. Jandus C, Boligan KF, Chijioke O, et al. Interactions between Siglec-7/9 receptors and ligands
555   influence NK cell-dependent tumor immunosurveillance. *J Clin Invest*. 2014;124(4):1810-1820.

556 37. zum Büschenfelde CM, Feuerstacke Y, Götze KS, et al. GM1 expression of non-Hodgkin's
557   lymphoma determines susceptibility to rituximab treatment. *Cancer Res.* 2008;68(13):5414-22.

558 38. Varki A. Since there are PAMPs and DAMPs, there must be SAMPs? Glycan "self-associated
559   molecular patterns" dampen innate immunity, but pathogens can mimic them. *Glycobiology*.
560   2011;21(9):1121-1124.

561 39. Stanczak MA, Siddiqui SS, Trefny MP, et al. Self-associated molecular patterns mediate
562   cancer immune evasion by engaging Siglecs on T cells. *J Clin Invest*. 2018;128(11):4912-
563   4923.

564 40. Haas Q, Boligan KF, Jandus C, et al. Siglec-9 regulates an effector memory CD8^{+} T-cell
565   subset that congregates in the melanoma tumor microenvironment. *Cancer Immunol Res.*
566   2019;7(5):707-718.

567 41. Soliman C, Yuriev E, Ramsland PA. Antibody recognition of aberrant glycosylation on the
568   surface of cancer cells. *Curr Opin Struct Biol*. 2017;44:1-8.

569 42. Galili U. Natural anti-carbohydrate antibodies contributing to evolutionary survival of primates
570   in viral epidemics? *Glycobiology*. 2016;26(11):1140-1150.

571 43. Griesemer A, Yamada K, Sykes M. Xenotransplantation: immunological hurdles and progress
572   toward tolerance. *Immunol Rev*. 2014;258(1):241-258.

573 44. Lai L, Kolber-Simonds D, Park KW, et al. Production of alpha-1,3-galactosyltransferase
574   knockout pigs by nuclear transfer cloning. *Science*. 2002;295(5557):1089-1092.

575 45. Phelps CJ, Koike C, Vaught TD, et al. Production of alpha 1,3-galactosyltransferase-deficient
576   pigs. *Science*. 2003;299(5605):411-414.

577 46. Sitaru C, Kromminga A, Hashimoto T, Brocker EB, Zillikens D. Autoantibodies to type VII
578   collagen mediate Fcgamma-dependent neutrophil activation and induce dermal-epidermal
579   separation in cryosections of human skin. *Am J Pathol*. 2002;161(1):301-311.

580 47. de Graauw E, Sitaru C, Horn M, et al. Evidence for a role of eosinophils in blister formation in
581   bullous pemphigoid. *Allergy*. 2017;72(7):1105-1113.

582 48. Cohen IR. Real and artificial immune systems: computing the state of the body. *Nat Rev
583   Immunol*. 2007;7(7):569-574.

584   49. Rieckmann JC, Geiger R, Hornburg D, et al. Social network architecture of human immune
585   cells unveiled by quantitative proteomics. *Nat Immunol.* 2017;18(5):583-593.

586   50. Cohen IR. The cognitive paradigm and the immunological homunculus. *Immunol Today.*
587   1992;13(12):490-494.

588   51. Macauley MS, Crocker PR, Paulson JC. Siglec-mediated regulation of immune cell function in
589   disease. *Nat Rev Immunol.* 2014;14(10):653-666.

590   52. Mortaz E, Tabarsi P, Mansouri D, et al. Cancers related to immunodeficiencies: update and
591   perspectives. *Front Immunol.* 2016;7:365.

592   53. Santos-Silva F, Fonseca A, Caffrey T, et al. Thomsen-Friedenreich antigen expression in
593   gastric carcinomas is associated with MUC1 mucin VNTR polymorphism. *Glycobiology.*
594   2005;15(5):511-7.

595   54. Mereiter S, Polom K, Williams C, et al. The Thomsen-Friedenreich Antigen: A Highly
596   Sensitive and Specific Predictor of Microsatellite Instability in Gastric Cancer. *J Clin Med.*
597   2018;7(9):256.

598   55. Agre P, Bertozzi C, Bissell M, et al. Training the next generation of biomedical investigators in
599   glycosciences. *J Clin Invest.* 2016;126(2):405-408.

600   56. Picard C, Bobby Gaspar H, Al-Herz W, et al. International Union of Immunological Societies:
601   2017 primary immunodeficiency diseases committee report on inborn errors of immunity. *J
602   Clin Immunol.* 2018;38(1):96-128.

603

604

605

606

607

608

609 **FIGURE LEGENDS**

610 **Figure 1. Antibody repertoire profiling on CFG and NCFGv2 glycan arrays**

611 **reveals broad carbohydrate recognition defects in symptomatic primary**

612 **antibody deficiencies (PADs). (A)** Glycan-specific binding of serum IgG screened

613 at 180 μg/ml on CFG glycan array version 5.1 (610 glycans) depicted as relative

614 fluorescence units (RFU). Screened sera were from cohorts with symptomatic

615 hypogammaglobulinemia (HGG; n=76), specific antibody deficiency (SPAD; n=5),

616 common variable immunodeficiency (CVID; n=25), CVID with low PPV vaccination

617 response (CVID PPV[low]; n=6), IgG subclass deficiency (IgGSD; n=8), or healthy

618 donors (HD; n=43). Significant values are reported, Kruskal–Wallis test. **(B)** Glycan-

619 binding reactivity matrices for individual sera (HD: n=12; SPAD: n=5; IgGSD: n=8;

620 HGG: n=11; CVID: n=12) screened on the NCFGv2 array and computed by the

621 dendrogram clustering algorithm as outlined in Materials and Methods. The color key

622 and distribution histogram are depicted. Columns represent the antibody reactivity

623 profiles (reactivity of each specific glycan for the different sera samples), and the

624 rows reflect the immune profiles for each patient subgroup, based on the mean

625 relative fluorescent units (RFU) values.

626 **Figure 2. Recognition of bacterial carbohydrate epitopes in PADs. (A)**

627 Spearman's rank correlation matrix for IgG recognition of pooled sera to all 121

628 bacterial carbohydrate structures identified by BCSDB analysis on the CFG array.

629 **(B,C)** Recognition of bacterial glycans by individual sera screened on the NCFGv2

630 array. **(B)** Dendrogrammed reactivity matrix based on the mean RFU values for all 65

631 glycans identified by BCSDB analysis. The color keys and distribution histograms are

632 depicted. **(C)** Heatmap presentation of glycan-specific IgG binding to selected

633 epitopes from *S. pneumoniae* (n=2), *H. influenzae* (n=3), *N. meningitidis* (n=6), *E. coli*

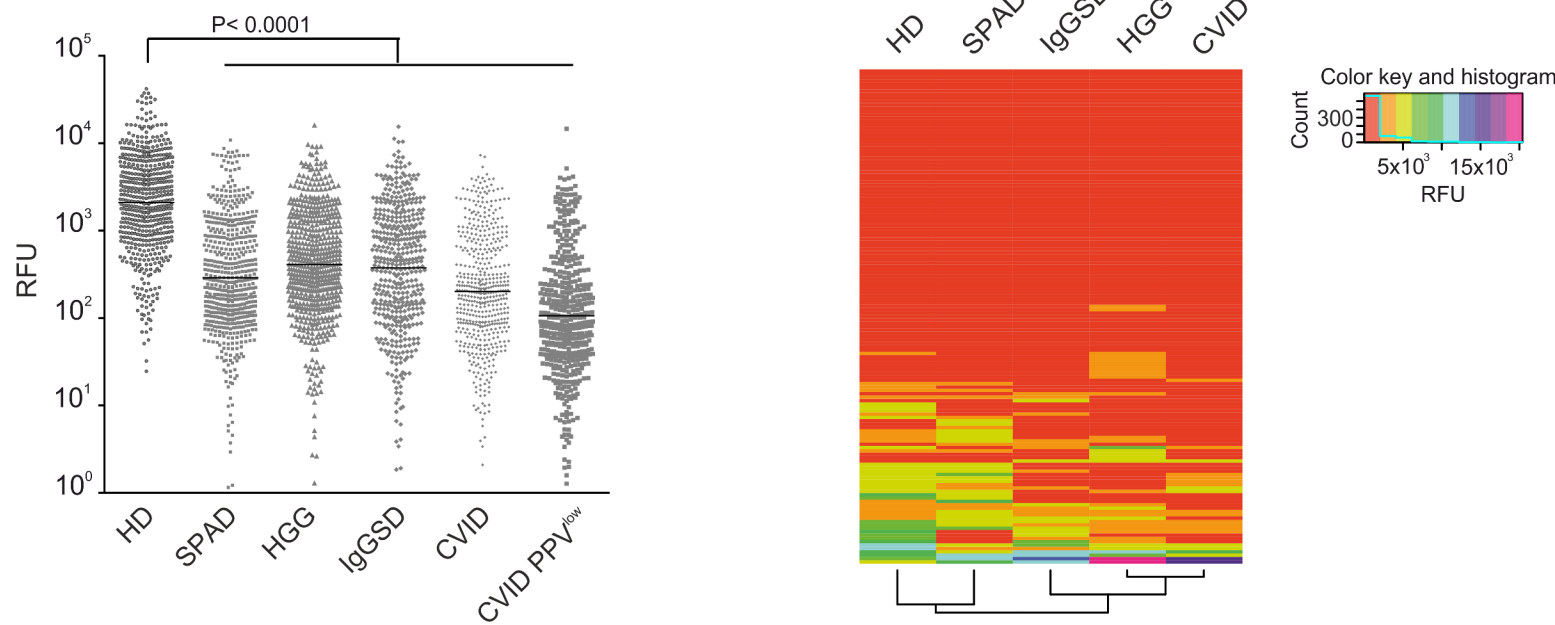634 (n=15), *H. pylori* (n=15), and *Salmonella* (n=2) species.

635 **Figure 3. Recognition of tumor-associated carbohydrates (TACAs) by glycan-**

636 **specific IgG in PAD. (A, B)** Recognition of TACAs by pooled serum IgG as

637 screened on the CFG array and depicted as dendrogrammed glycan reactivity matrix

638 based on ABR **(A)**, or as radial dendrogram based on RFU values **(B)**. **(C)** Heatmap

639 presentation based on RFU values illustrating reactivity of individual serum IgG to

640 TACAs as revealed by screening on the NCFGv2 array. The color keys and

641 distribution histograms are depicted.

642 **Figure 4. Deviant recognition of distinct terminal carbohydrate moieties and**

643 **specific loss of Galα reactivity in symptomatic PAD. (A)** Binary deviation map (P

644 < 0.05) of IgG immunoprofiles compared to healthy controls based on two-way

645 ANOVA and hierarchical clustering analysis with identification of cliques 1-4. The

646 rows in this matrix indicate the binary antibody reactivity profiles, and the columns

647 represent the deviation immune profiles for each PAD subgroup. **(B)** Terminal

648 carbohydrate moieties of epitopes in reactivity cliques 2 (non-significant deviation)

649 and 4 (significant deviation). Numeric occurrence is indicated in parenthesis. **(C, D)**

650 Recognition of Galα- **(C)** or GalNAc- **(D)** epitopes within clique 4 (significant

651 deviation). **(E)** Deviation map based on degree of significance with identification of

652 cliques A-E. **(F)** Bubble chart displaying terminal glycan structure distribution across

653 cliques A-E. The size key and percentage numbers indicate frequencies.

654 **Figure 5. Diminished recognition of Galα-terminated glycan epitopes and**

655 **reduced Galα-dependent xenogeneic anti-porcine reactivity of CVID and**

656 **symptomatic IgGSD sera. (A)** IgG antibody reactivity to Galili, αLN and Aα3GN

657 glycans as assessed by suspension array (multiplex immunoassay). Individual sera

658 from healthy donors (n=18), HGG patients (n=37), CVID (n=15) and IgGSD (n=8)

659 patients were analyzed. Box-and-whisker diagrams were created by the Tukey

660 method. The middle line is plotted at the median and the box represents the

661 interquartile range (difference between the 25th and 75th percentiles). Significant

662 values are reported, Kruskal–Wallis test. **(B)** Reduced surface staining of anti-Galili

663 mAb reactivity following α-galactosidase treatment of porcine PK15 cells, as

664 assessed by flow cytometry. Representative histogram (left panel) and summary

665 (right panel). **(C)** Antibody dependent cellular cytotoxicity (ADCC) activity of primary

666 human NK cells against PK15 cells at E/T ratio of 10:1, in absence or presence of α-

667 galactosidase. Significant values are reported (Student's *t*-test). **(D)** Histopathologic

668 analysis of pig skin damage in cryosections incubated with healthy and patient sera

669 in presence of healthy human leukocytes. Representative examples for each

670 analyzed disease and control (PBS) are shown (left panel). The dashed lines indicate

671 the dermal-epidermal junction. Pictures were taken with 40X magnification, scale

672 bars 75μm. The damage induced was calculated as the dermal-epidermal separation

673 normalized to the IgG concentration in the sera (right panel) (at least n=7). Results

674 are representative of at least three **(C)** or seven **(D)** experiments. Significant values
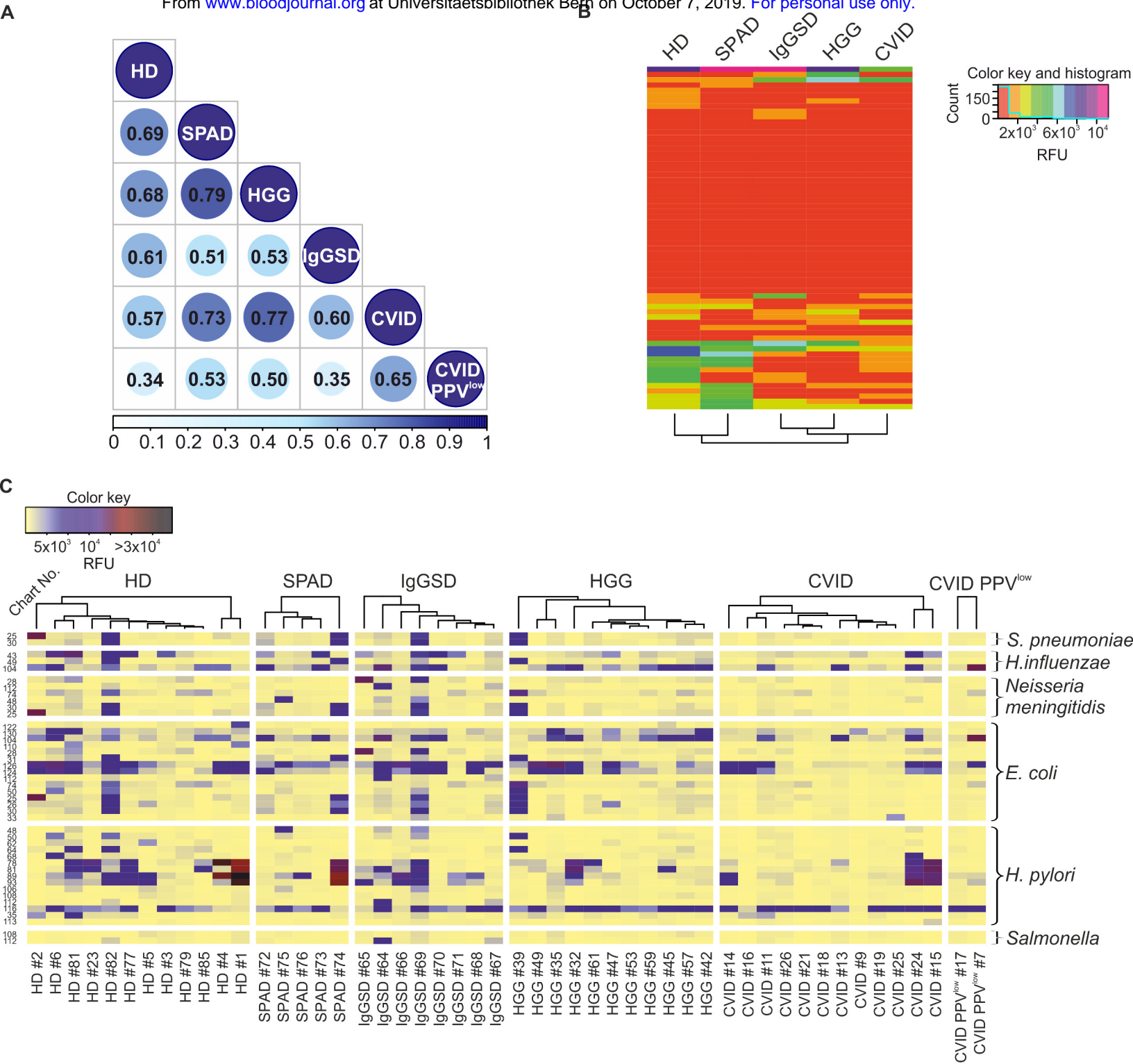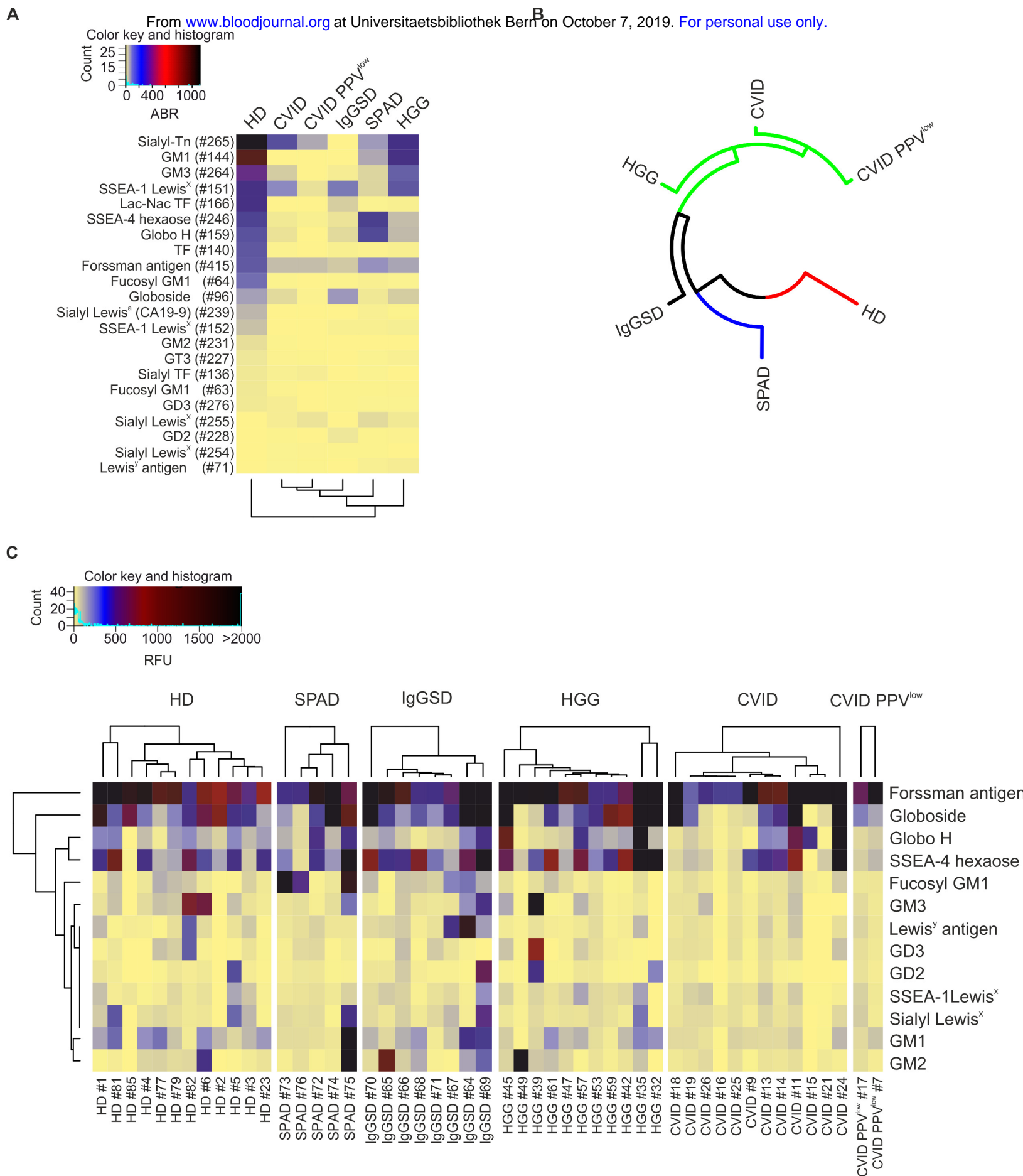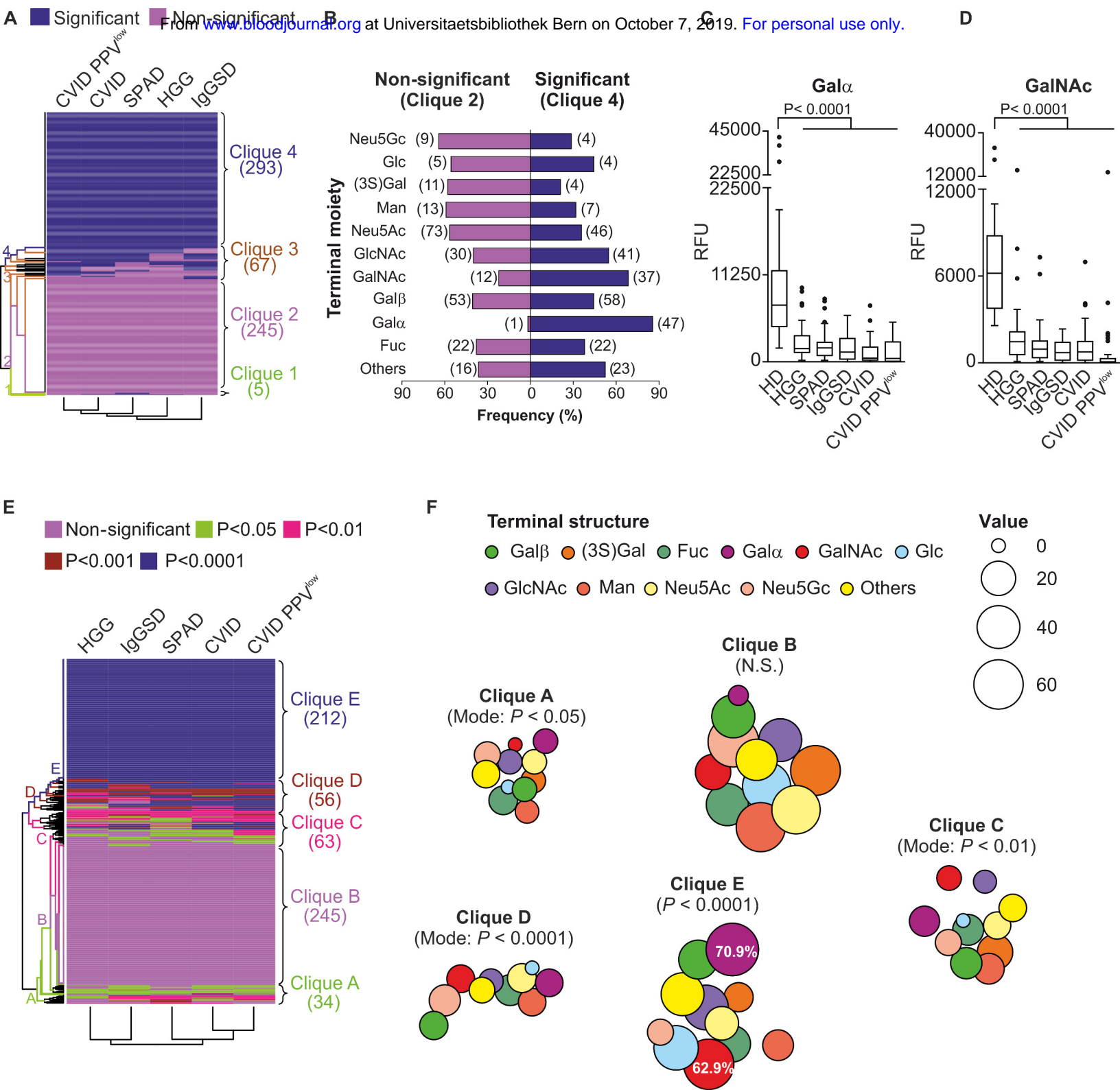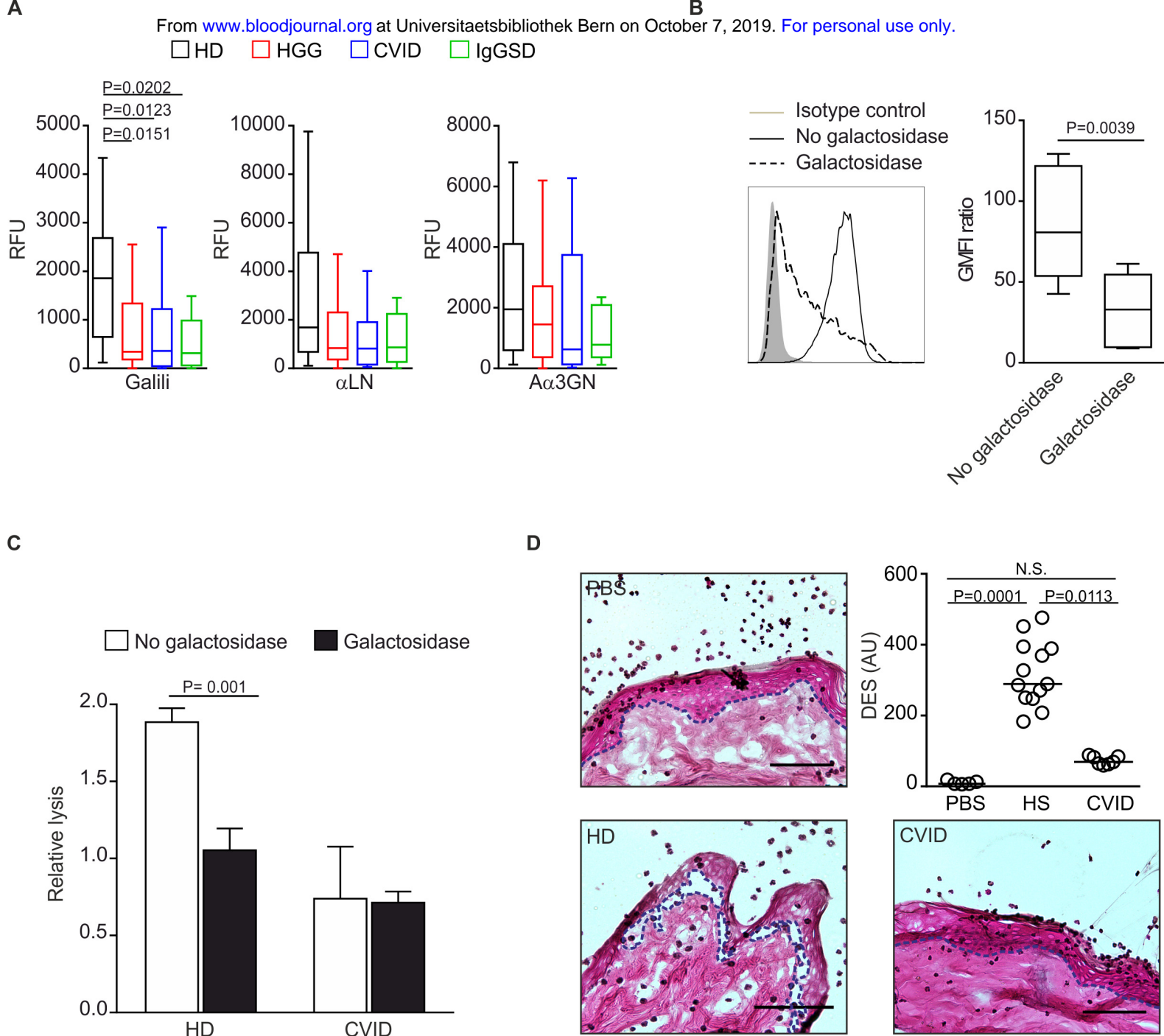
675 are reported (Kruskal–Wallis test).

676

A

B

Figure 1

Figure 2

Figure 3

A

B

C Galα

D GalNAc

E

F

Figure 4

A

□ HD □ HGG □ CVID □ IgGSD

B

C

D

Figure 5

The architecture of the IgG anti-carbohydrate repertoire in primary antibody deficiencies (PADs)

Peter Jandus, Kayluz Frias Boligan, David F. Smith, Elisabeth de Graauw, Bodo Grimbacher, Camilla Jandus, Mai M. Abdelhafez, Alain Despont, Nicolai Bovin, Dagmar Simon, Robert Rieben, Hans-Uwe Simon, Richard D. Cummings and Stephan von Gunten